Journal of Applied Polymer Science

Highly Antibacterial and Toughened Polystyrene Composites with Silver Nanoparticles Modified Tetrapod-Like Zinc Oxide Whiskers

Xiaoyong Pan, Ling Peng, Yong Liu, Jie Wang
Engineering and Technology Center, Sichuan Changhong Electric Co., Ltd., Mianyang, Sichuan 621000, China
Correspondence to: J. Wang (E-mail: wjxfm1@gmail.com)

ABSTRACT: In this work, high-performance multifunctional composites were obtained by melt blending silver deposited tetrapod-like zinc oxide whiskers (Ag-ZnOw) with polystyrene (PS). The chemical, spectroscopic, antibacterial, mechanical, and morphological properties of the PS/Ag-ZnOw composites were carefully investigated and discussed. The obtained PS/Ag-ZnOw composites characterized remarkable antibacterial activity against *Escherichia coli* (*E. coli*) and *Staphylococcus aureus* (*S. aureus*). Moreover, it is found that impact strength of the composite increase with increasing nanofiller concentration (up to 0.25 wt %). Morphological characterization of the impact fractured surface of composites revealed that toughening was achieved through uniform filler distribution in the polymer matrix, and anchoring effect was imparted by the tetrapod-like shape of ZnO whiskers. © 2014 Wiley Periodicals, Inc. J. Appl. Polym. Sci. **2014**, *131*, 40900.

KEYWORDS: composites; mechanical properties; nanoparticles; nanowires and nanocrystals; polystyrene

Received 10 November 2013; accepted 18 April 2014
DOI: 10.1002/app.40900

INTRODUCTION

Polystyrene (PS) is a transparent, nontoxic, mechanically adequate, and easy-processing material that can be used to make electronic equipment housing, disposable kitchen utensils and compact discs, etc. However, despite being operated at low temperatures, refrigerator trays made of PS can be hot spots for bacteria.[1] Previous study found that the concentration of viable cells in refrigerators is around $\log_{10}$ 7.1 colony-forming units (CFU) per cm^2 in average. Moreover, more than half of the inspected refrigerators contained pathogenic microorganisms.[2] So, it is very important to protect consumer health by preventing cross-contamination through contaminated surfaces.[3] On the basis of the aforementioned considerations, PS becomes increasingly less appealing for refrigeration trays manufactures, and a mechanically stronger replacement for PS with antibacterial property is thus needed. Several researches have been done to either toughen PS,[4–6] or incorporate antibacterial property to PS,[7–10] while very few researches have managed to incorporate both properties by adding one type of filler particles. Wang et al.[11] and Zhang et al.[12] used TiO_2 as toughening and antibacterial agent and both of them found that the maximum of impact strength and antibacterial activity appeared with the addition of 1.0 wt % TiO_2. Although enhancements in both properties were observed in these aforementioned studies, further optimization can be realized by tailoring the composition, shape, and surface properties of nanofillers.

More and more photocatalytic researches focus on ZnO instead of TiO_2 due to the higher efficiency of ZnO in generating, moving and separating photoinduced electrons and holes.[13] Similar to TiO_2, ZnO can be used to simultaneously improve mechanical and antibacterial property of polymer composites.[14–16] However, the extent of improvement is somewhat limited. Taking the antibacterial rates of polymer composites against *E. coli* as an example, Li et al. found that 4 wt % ZnO nanoparticles was needed to achieve 90% antibacterial rate,[17] Ma et al. found that it took 1.5 wt % ZnO nanowhiskers to achieve more than 90% antibacterial rate,[18] Li et al. achieved 98.4% antibacterial rate upon 1 wt % ZnO nanoparticle incorporation.[19] In general, it takes at least 1 wt % ZnO filler to produce polymer composites with 98% antibacterial rate. At high filler concentration, particles usually formed stress-concentrating aggregates in the polymer matrix, consequently weakening the composites. Moreover,

Contribution of each author: Dr. Xiaoyong Pan carried out some of the experiments, and wrote this manuscript. Mrs. Ling Peng helped take SEM pictures and provided critical suggestions about the analysis of SEM tests. Mr. Yong Liu helped with mechanical testing, and helped with the explanation of enhanced mechanical property. Mrs. Jie Wang also carried out some of the experiments and helped devising the entire research.

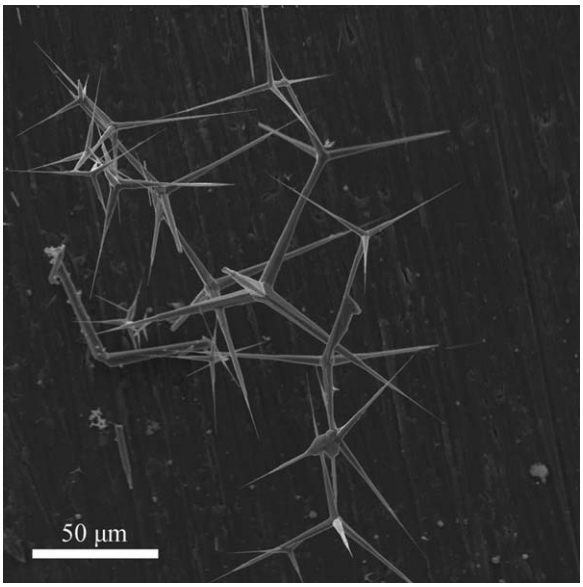

Figure 1. SEM image of typical pure ZnOw.

composites with high filler concentration can be very expensive to fabricate, and difficult to process as well. Numerous attempts were made to solve this aforementioned problem, and later researches showed that the filler concentration can be reduced by altering the shape of particles.[20,21] It was found that tetrapod-like ZnO whiskers (ZnOw) exhibit better antibacterial efficiency than other regular-shaped ZnO nanoparticles, thanks to the unique tetrapod-like structure that prevents aggregation of nanoparticles and enables quantum effects at whisker tips.[20] Besides controlling the shape of nanofillers, it was possible to improve antibacterial activity of the semiconducting ZnO nanofillers by improving their photocatalytic property.[11] Among the numerous methods used to enhance photocatalytic activity, three most popular methods are semiconductor combination,[22,23] transition metals deposition,[24,25] and noble metal deposition.[26,27] Previous study showed that silver nanoparticle deposition could be used to modify ZnOw, leading to better photocatalytic property.[28]

In this study, pure ZnOw were first modified with silver nanoparticles using photodeposition, and then the obtained Ag-ZnOw nanofillers were incorporated into PS matrix via melt-blending to produce multifunctional Ag-ZnOw/polymer nanocomposites with low filler concentration (no more than 0.25 wt %). The antibacterial and mechanical properties of the nanocomposites were found to increase with increasing filler concentration.

EXPERIMENTAL

Materials

General purpose polystyrene with a density of 1.05 g cm^{-3} and a melt flow rate of 3 g/10 min (200°C, 5 kg) was purchased from BASF-YPC (158 K, Nanjing, China). Tetrapod-like zinc oxide whiskers was synthesized by the equilibrium gas expanding method using the metallic zinc powders as the main raw material at 700°C.[29] The average length of the ZnOw whiskers was 20–50 μm and the density of ZnOw was 6.76 g cm^{-3}, as shown in Figure 1. Analytical grade silver nitrate ($AgNO_3$) and polyethylene glycols (PEG) were used as received. Deionized water was used to prepare all the solutions in this article.

Preparation of PS/Ag-ZnOw

Ag-ZnOw nanoparticles were prepared according to the procedures described in our previous publication,[28] and the TEM image of obtained Ag-ZnOw nanocompound was shown in Figure 2. It can be seen that Ag nanoparticles were successfully deposited on the surface of ZnO whiskers with particle size ranging from 50 to 100 nm. The obtained Ag-ZnOw were then mixed with PS to produce PS/Ag-ZnOw nanocomposites using the following procedure: firstly, PS pellets and Ag-ZnOw nanoparticles were dried in oven for 6 h at 60 and 80°C, respectively, and then the nanoparticles were mixed with PS pellets using a twin screw extruder at a weight ratio of 1:100 to prepare master batch. The temperatures of the extruder from the feeding zone to the die were set at 170, 190, 200, and 195°C and the screw speed was set at 40 rpm (TSSJ-25, China). Second, the master batch was diluted by melt mixing with pure PS using the same processing conditions to produce samples with different Ag-ZnOw nanoparticle concentrations (0, 0.05, 0.15, and 0.25 wt %). Extruded pellets of all the samples were fabricated into standard testing bars using an injection-molding machine (NISSE I-PS40E5ASE, Japan) at a melting temperature of 200°C and a molding temperature of 40°C.

Characterization

Inductively Coupled Plasma Emission Spectrometer (ICP). The concentration of Ag in PS/Ag-ZnOw nanocomposites was analyzed by inductively coupled plasma emission spectrometer (Thermo iCAP6300).

Scanning Electron Microscopy (SEM). Scanning electron microscope (Philips-FEI, XL30) was employed to examine the morphology of the gold plated surfaces of impact fractured samples.

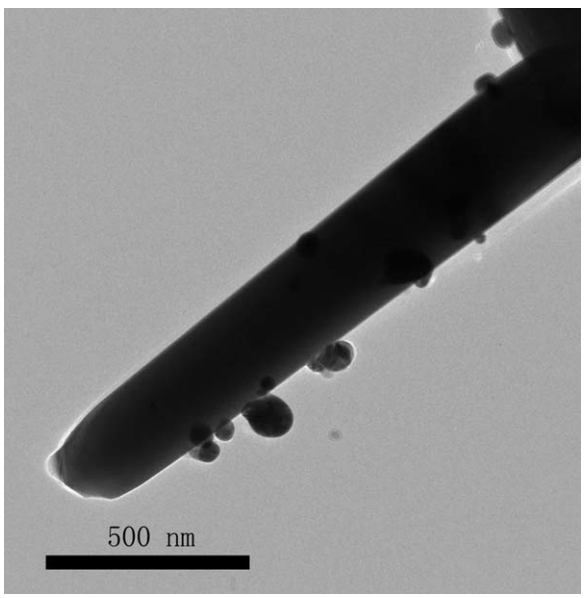

Figure 2. TEM image of Ag-ZnOw nanocompound.

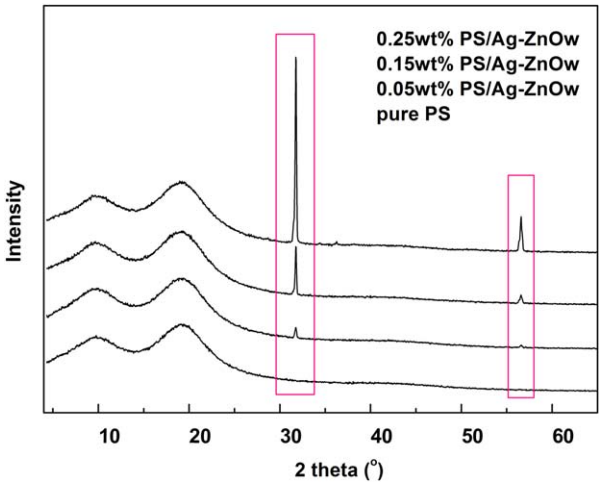

Figure 3. XRD patterns of pure PS, and PS/Ag-ZnOw nanocomposites prepared with Ag-ZnOw contents of 0.05, 0.15, and 0.25 wt %. [Color figure can be viewed in the online issue, which is available at wileyonlinelibrary.com.]

Transmission Electron Microscopy (TEM). The morphology of Ag-ZnOw nanocompound was studied using transmission electron microscopy (JEOL, 2010F).

Ultraviolet-Visible Spectroscopy (UV-vis). The absorbance spectra of samples from 200–800 nm were obtained by a UV-vis spectrophotometer (Shimadzu, 2550).

Mechanical Properties Measurements. Notched Izod impact strength was measured using an impact tester (XC-22Z, China) according to ISO180–2000. The reported impact strength was the average of five measurements.

Wide Angle X-ray Diffraction (WAXD). The crystalline structure of samples was investigated using a WAXD (Panalytical X'pert PRO diffractmeter with Ni-filtered Cu Kα radiation, the Netherlands). The continuous scanning angle used in this work was from 0° to 70° at 40 kV and 40 mA.

Antibacterial Experiments. The antibacterial property against *Escherichia coli* (*E. coli*) and *Staphylococcus aureus* (*S. aureus*) were determined independently by Guangdong Detection Center of Microbiology according to GB 21551.2–2010.[30] The samples (5×5 cm^2) were first washed with 75% ethanol to kill all bacteria on the surface. After drying, a 0.2 mL solution of bacteria ($2.0–5.0 \times 10^5$ CFU mL^{-1}) was added onto the film surface. These carrier films were kept at 37°C and at a relative humidity of 90% or greater. After 24 h, the bacteria were washed off with a 0.80% NaCl solution, and then, a 1mL serial dilution of this suspension was plated onto nutrient broth agar. The samples were kept at 37°C for another 24 h before counting the colony forming units of bacteria according to GB 4789.2–2010,[31] and the antibacterial rate (R) was calculated with the following equation[32,33]:

$$R = \frac{B - C}{B} \times 100\% \quad (1)$$

where B is the number of colony forming units of the blank sample (with 0 wt % filler concentration) and C is the number of colony forming units of the antibacterial samples. Every reported antibacterial rate (for each bacterial) is an average of three measurements. It should be noted that the effect of natural light irradiation on antibacterial efficiency was tested. For samples tested with natural light, there is no extra measure to prevent light irradiation. For samples tested in the dark, natural light irradiation was shielded using aluminum foil.

RESULTS AND DISCUSSION

Composition Characterization

The XRD patterns of the pure PS and PS/Ag-ZnOw compound prepared with different Ag-ZnOw contents are shown in Figure 3. It can be seen that the diffraction peaks at $2\theta = 19.06°$ can be attributed to PS,[34] and the $2\theta = 31.88°$ and 56.62° are assigned to the (100) and (110) planes of wurtzite structure of ZnO crystals (JCPDS file no. 36-1451).[35] The intensity of the diffraction peaks of ZnO increases with the increasing Ag-ZnOw content, as shown in the red rectangles in Figure 3. However, no diffraction peaks of metallic Ag can be detected due to the large ZnOw/Ag ratio (Ag deposited as nanoparticles on ZnOw surface). Besides, the incorporation of Ag-ZnOw nanoparticles produces neither a new peak nor a shift with respect to PS, indicating the absence of any crystalline impurities within PS/Ag-ZnOw composites. To further determine the existence of Ag in the composites, ICP test was conducted. It is shown that for PS/Ag-ZnOw samples with 0.05, 0.15, and 0.25 wt% filler concentrations, the content of Ag were 9, 14, and 32 ppm, respectively.

Antibacterial Activity

The antibacterial activities of the synthesized nanocomposites against *E. coli* and *S. aureus* were studied and the results are shown in Table I. While pure PS has no antibacterial activity, the antibacterial efficiency of PS/Ag-ZnOw nanocomposites increased with increasing Ag-ZnOw nanoparticles content. Upon addition of only 0.05 wt % Ag-ZnOw nanoparticles, the antibacterial efficiency of the composites are already as high as 91.35% against *E. coli* and 92.56% against *S. aureus*, satisfying the antibacterial standard for the electric home appliance of China.[30] Further increasing Ag-ZnOw content to 0.25 wt % pushes the antibacterial efficiency to 99.99% against both *E. coli* and *S. aureus*. This result is remarkably better than previous researches, which showed 99% antibacterial efficiency only after incorporation of 1 wt % TiO_2,[11,12] or 0.8 wt % ZnO.[36] To clarify the antibacterial mechanism of PS/Ag-ZnOw nanocomposites, the antibacterial efficiency was further tested under no light condition. Without

Table I. Antibacterial Efficiency of Pure PS, and PS/Ag-ZnOw Nanocomposites Under Different Testing Conditions

Ag-ZnOw nanoparticles (wt %)	Experimental condition	Antibacterial rate (%)	
		E. coli	*S. aureus*
0	Natural light	0	0
0.05	Natural light	91.35	92.56
0.15	Natural light	97.99	99.99
0.25	Natural light	99.99	99.99
0.25	No light	88.33	99.52

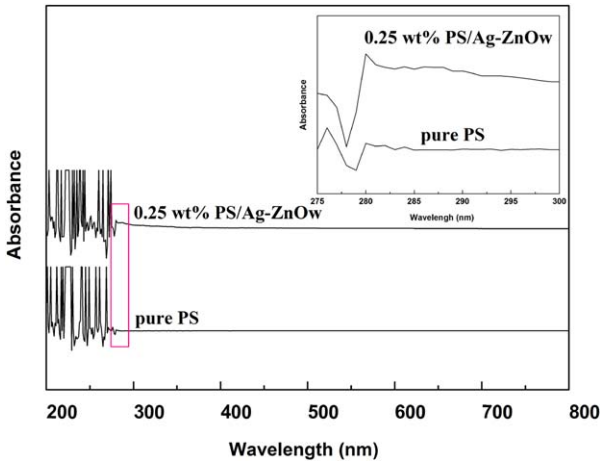

Figure 4. UV–vis spectra of pure PS, and PS/Ag-ZnOw nanocomposites prepared with 0.25 wt % Ag-ZnOw. [Color figure can be viewed in the online issue, which is available at wileyonlinelibrary.com.]

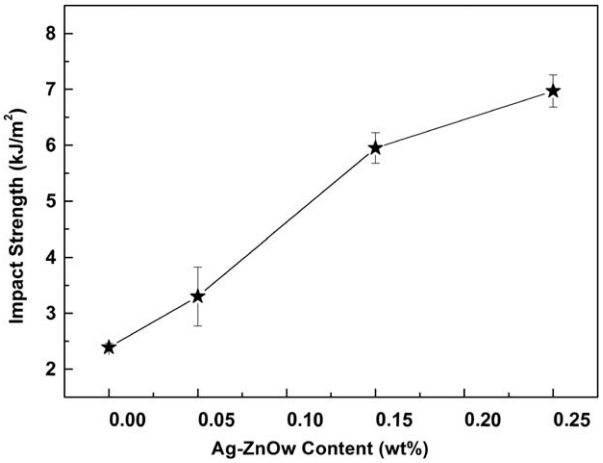

Figure 5. Effect of filler contents on impact strength of PS/Ag-ZnOw nanocomposites.

natural light irradiation, the antibacterial efficiency of sample with 0.25 wt % filler concentration were slightly decreased to 88.33 and 99.52% for *E. coli* and *S. aureus*, respectively.

Antibacterial Mechanism

The antibacterial activity of Ag, ZnO, and their corresponding nanocomposites has been extensively investigated.[37–42] The most widely accepted antibacterial mechanisms are: (1) active oxygen generation, which requires light irradiation,[43,44] and (2) hydrogen peroxide (H_2O_2) generation, which doesn't require light irradiation.[45] By conducting experiment in the dark, the generation of active oxygen through photocatalytic process can be inhibited, allowing us to study the effect of H_2O_2 separately. It is reported that H_2O_2 can inhibit the growth or even kill the bacteria by damaging the cell membrane of bacteria through oxidization.[45] As described in the previous section, the antibacterial efficiency for samples tested in the dark decreased slight from 99.99 to 88.33% for *E. coli*, and from 99.99 to 99.52% for *S. aureus*. This result indicates that the active oxygen generated by photocatalytic activity plays a less important role in antibacterial mechanism. Therefore, the generation of H_2O_2 from Ag-ZnOw is considered as the primary cause for antibacterial activity of PS/Ag-ZnOw nanocomposites.

On the other hand, it worth pointing out that despite being less important than H_2O_2, active oxygen generated under light irradiation does function synergistically, and further increases the antibacterial efficiency to 99.99% for both *E. coli* and *S. aureus*. So, the antibacterial mechanism of active oxygen deserves some explanation. When semiconducting ZnO is subjected to light irradiation, electron-hole pairs can be generated on its surface. Subsequently, the hole (h^+) can react with OH^- on the surface to generate hydroxyl radicals (OH•), superoxide anion (O_2^-) and perhydroxyl radicals (HO_2•).[46] These highly active free radicals could disrupt the cell wall of microorganism as a result of decomposition.[47,48] Incorporation of Ag onto the surface of ZnO will further improve the charge transfer, reduce the recombination rate of electron-hole pairs, and ultimately promote the generations of perhydroxyl radicals and other strong oxidizing materials.[49,50] In general, semiconducting materials with stronger absorption in UV region have better photocatalytic and antibacterial activity.[11] Therefore, UV–vis spectra were obtained to verify the photocatalytic and antibacterial activity of the PS/Ag-ZnOw nanocomposites. The UV–vis spectra of neat PS, and PS/Ag-ZnOw nanocomposites prepared with 0.25 wt % Ag-ZnOw content are shown in Figure 4. It can be seen that both samples show a limited UV absorbance in the range of 200–300 nm. However, a close look at the 275–300 nm wavelength region (outlined by red rectangle) reveals remarkably different absorption characteristics, as shown in the inset of Figure 4. Addition of 0.25 wt % Ag-ZnOw nanoparticles enhanced the UV absorption at 280 nm due to the intrinsic wide band gap of ZnOw, and then reduced exciton binding energy of Ag-ZnOw nanocompound.[21] In all, the antibacterial mechanism of PS/Ag-

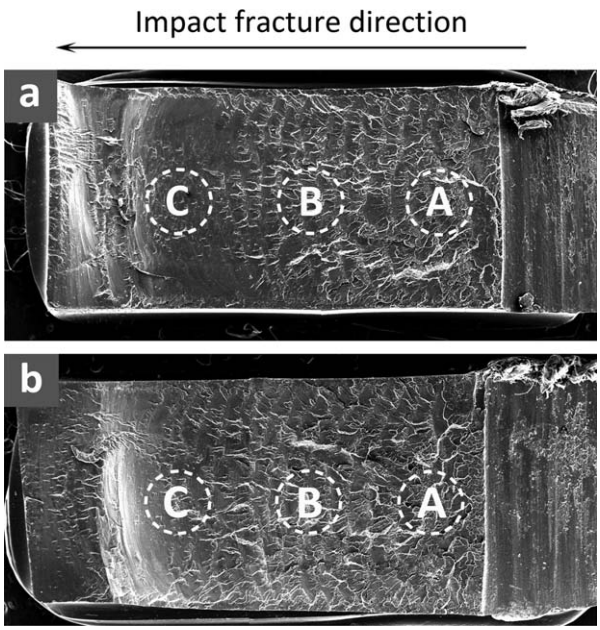

Figure 6. SEM images showing impact fractured surfaces of pure PS (a), and PS/Ag-ZnOw nanocomposite with 0.25 wt % Ag-ZnOw (b) at different zones. The arrow shows the impact fracture direction.

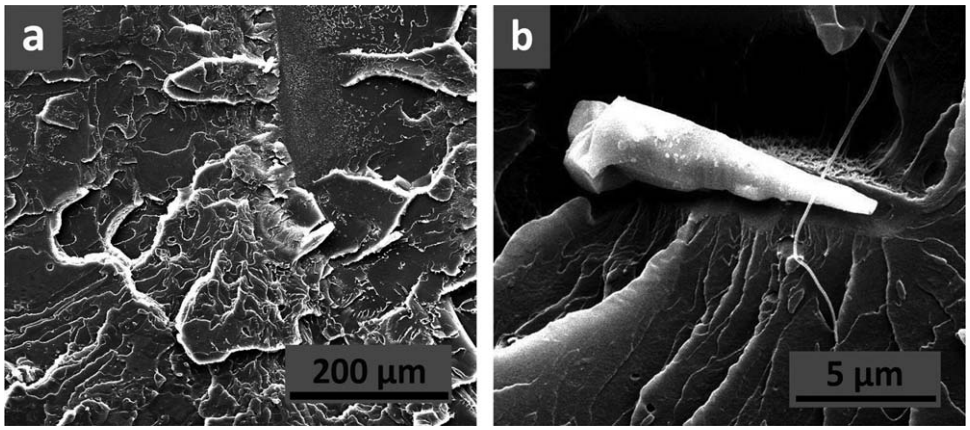

Figure 7. SEM images in zone C of PS/Ag-ZnOw nanocomposite with 0.25 wt % Ag-ZnOw at medium (a), and high (b) magnifications.

ZnOw composites originate from both active oxygen and H_2O_2, with H_2O_2 being the primary factor.

Mechanical Property

The influence of Ag-ZnOw nanofillers content on impact strength is shown in Figure 5. It is found that the impact strength of PS/Ag-ZnOw composites increased with increasing Ag-ZnOw content. The impact strength of PS (2.38 kJ m^{-2}) was tripled upon addition of 0.25 wt % Ag-ZnOw (7.21 kJ m^{-2}). Similar researches using $CaCO_3$ or SiO_2 to toughen PS exhibit only limited level of enhancement,[51,52] due to a lot of factors, such as filler aggregation, or insufficient energy transfer between polymer matrix and inorganic filler. Compared with these researches, advantage of using Ag-ZnOw nanofillers is indeed remarkable.

To clarify the toughening effect of ZnOw, impact fractured surfaces of pure PS, and PS/Ag-ZnOw nanocomposite with 0.25 wt % filler concentration were characterized using SEM. As shown in Figure 6, both samples have relatively rough surface in crack initiation zone (zone A) and crack propagation zone (zone B), indicating adequate impact energy absorption. However, different surface morphologies can be observed at the crack propagation zone (zone C). Pure PS specimen has a relatively smooth surface at this zone, indicating insufficient impact energy absorption during high speed fracture. On the contrary, zone C of PS/Ag-ZnOw nanocomposite exhibit rougher surface (a typical feature of efficient energy adsorption), which corresponds well with the higher impact energy of nanocomposite.

The propagation zone [zone C in Figure 6(b)] of the nanocomposite was further characterized at medium and high magnifications (shown in Figure 7) to determine the dispersion and toughening mechanism of T-ZnOw. As can be seen in Figure 7(a), there are no stress-concentrating filler agglomerates in the PS matrix, and the uniform dispersion of nanoparticles within the matrix could facilitate more plastic deformation than that in pure PS. As pointed out by Nakagawa et al.,[53] uniform dispersion of filler increases the critical stress needed to initiate microcracks during the fracture of nanocomposites. The consequent plastic deformation around the nanoparticles will absorb more impact energy.[11] Moreover, pull out effect was observed in Figure 7(b). It is reported that during the pulled out of tetrapod ZnO whisker, only one or two needles of the particle may be pulled out due to the unique three dimensional tetrapod structure, while the other embedded needles can exert anchoring force on crack, leading to impeded crack propagation, finally leading to more severe plastic deformation and more efficient energy absorption.[54]

CONCLUSIONS

In this article, PS/Ag-ZnOw nanocomposites with excellent antibacterial and mechanical properties were successfully fabricated. The incorporation of Ag-ZnOw nanoparticles in the PS was firstly confirmed by XRD and ICP tests. Thanks to the superior photocatalytic property of Ag-ZnOw compound over conventional photocatalytic nanoparticles, PS/Ag-ZnOw nanocomposites exhibit better antimicrobial property against *E. coli* and *S. aureus* than other conventional antimicrobial composites. The impressive antibacterial property originates from both active oxygen and H_2O_2, with H_2O_2 being the primary factor. Addition of Ag-ZnOw nanoparticles was found to improve the impact strength of PS, and the extent of enhancement increased with increasing filler concentration. The impact fracture surfaces of pure PS and PS/Ag-ZnOw composites were compared to elucidate the toughening mechanism, and it was found the nanocomposite had a rougher crack propagation zone, indicating more efficient energy adsorption. Further analysis of the propagation zone at higher magnification reveals that the uniform distribution and unique tetrapod shape of the nanofillers contribute to more efficient energy adsorption, which ultimately leads to effective toughening.

ACKNOWLEDGMENTS

The authors thank the National High Technology Research and Development Program of China (No. 2013AA040207 and No. 2013AA041305) for providing the research grant.

REFERENCES

1. Bielecki, J. *Acta Microbiol. Polym.* **2003**, *52*, 17.

2. Kennedy, J.; Jackson, V.; Blair, I. S.; McDowell, D. A.; Cowan, C.; Bolten, D. J. *J. Food Prot.* **2005**, *68*, 1421.
3. Kampmann, Y.; De Clerck, E.; Kohn, S.; Patchala, D. K.; Langerock, R.; Kreyenschmidt, J. *J. Appl. Microbiol.* **2008**, *104*, 1808.
4. Mathur, D.; Nauman, E. B. *J. Appl. Polym. Sci.* **1999**, *72*, 1151.
5. Ramar, P.; Alagar, M. *J. Appl. Polym. Sci.* **2009**, *111*, 2859.
6. Zhang, J. Z.; Wang, X.; Lu, L. D.; Li, D.; Yang, X. J. *J. Appl. Polym. Sci.* **2003**, *87*, 381.
7. Gao, B. J.; Qi, C. S.; Liu, Q. *Appl. Surf. Sci.* **2008**, *254*, 4159.
8. Nassar, M. A.; Youssef, A. M. *Carbohydr. Polym.* **2012**, *89*, 269.
9. Youssef, A. M.; Kamel, S. *Carbohydr. Polym.* **2013**, *98*, 1166.
10. Jiang, G. H.; Zeng, J. F. *J. Appl. Polym. Sci.* **2010**, *116*, 779.
11. Wang, Z. B.; Li, G. C.; Peng, H. R.; Zhang, Z. K. *J. Mater. Sci.* **2005**, *40*, 6433.
12. Zhang, Q. S.; Peng, H. R.; Zhang, Z. K. *J. Dispersion Sci. Technol.* **2007**, *28*, 937.
13. Li, Y. Z.; Xie,W.; Hu, X. L.; Shen, G. F.; Zhou, X.; Xiang, Y.; Zhao, X. J.; Fang, P. F. *Langmuir* **2010**, *26*, 591.
14. Sawai, J.; Igarashi, H.; Hashimoto, A.; Kokugan, T.; Shimizu, M. *J. Chem. Eng. Jpn.* **1995**, *28*, 288.
15. Sawai, J.; Saito, I.; Kanou, F.; Igarashi, H.; Hashimoto, A.; Kokugan, T.; Shimizu, M. *J. Chem. Eng. Jpn.* **1995**, *28*, 352.
16. Wang, Y.; Shi, J.; Han, L.; Xiang, F. M. *Mater. Sci. Eng. A* **2009**, *501*, 220.
17. Li, J. H.; Hong, R. Y.; Li, M. Y.; Li, H. Z.; Zheng, Y.; Ding, J. *Prog. Org. Coat.* **2009**, *64*, 504.
18. Ma, X. Y.; Zhang, W. D. *Polym. Degrad. Stab.* **2009**, *94*, 1103.
19. Li, S. C.; Li, Y. N. *J. Appl. Polym. Sci.* **2010**, *116*, 2965.
20. Duan, X.; Xu, X. L.; Huang, C.; Yi, Z. G.; Zhu, W. J.; Wang, L.; Zhou, Z. W.; Fan, X. M. *J. Funct. Mater.* **2010**, *41*, 496.
21. Yamamoto, O. *Int. J. Inorg. Mater.* **2001**, *3*, 643.
22. Xu, J.; Chang, Y.; Zhang, Y.; Ma, S.; Qu, Y.; Xu, C. *Appl. Surf. Sci.* **2008**, *255*, 1996.
23. Cao, Y.; Zhang, X.; Yang, W.; Du, H.; Bai, Y.; Li, T.; Yao, J. *Chem. Mater.* **2000**, *12*, 3445.
24. Xiao, Q.; Zhang, J.; Xiao, C.; Tan, X. *Mater. Sci. Eng. B* **2007**, *142*, 121.
25. Kim, D. H.; Choi, D.; Kim, S.; Lee, K. S. *Catal. Commun.* **2008**, *9*, 654.
26. Zhou, G.; Deng, J. *Mater. Sci. Semicond. Process.* **2007**, *10*, 90.
27. Wang, R.; Xin, J. H.; Yang, Y.; Liu, H.; Xu, L.; Hu, J. *Appl. Surf. Sci.* **2004**, *227*, 312.
28. Wang, J.; Fan, X. M.; Zhou, Z. W.; Tian, K. *Mater. Sci. Eng. B* **2011**, *176*, 978.
29. Zhou, Z. W.; Peng, W. M.; Ke, S. Y.; Deng, H. *J. Mater. Process. Technol.* **1999**, *89*, 415.
30. Zhang, T. Y. GB 21551.2-2010: General administration of quality supervision, inspection and quarantine of P.R.C. **2010**.
31. Liu, X. M. GB 4789.2-2010: National food safety standard-Food microbiological examination: Aerobic plate count, the Minister of Health of P.R.C. **2010**.
32. Zhang, W.; Chu, P. K.; Ji, J. H.; Zhang, Y. H.; Fu, R. K. Y.; Yan, Q. *Polymer* **2006**, *47*, 931.
33. Dong, X. X. QB/T2591-2003: National development and reform commission of P.R.C. **2003**.
34. Gaur, M. S.; Singh, P. K.; Chauhan, R. S. *J. Appl. Polym. Sci.* **2010**, *118*, 2833.
35. Wang, J.; Fan, X. M.; Tian, K.; Zhou, Z. W.; Wang, Y. *Appl. Surf. Sci.* **2011**, *257*, 7763.
36. Li, S. C.; Li, B.; Qin, Z. J. *Polym. Plast. Technol. Eng.* **2010**, *49*, 1334.
37. Li, Q.; Chen, S. L.; Jiang, W. C. *J. Appl. Polym. Sci.* **2007**, *103*, 412.
38. Perelshtein, I.; Ruderman, E.; Perkas, N.; Tzanov, T.; Beddow, J. *J. Mater. Chem. B*, **2013**, *1*, 1968.
39. Manna, J.; Begum, G.; Kumar, K. P.; Misra, S.; Rana, R. K. *Appl. Mater. Interfaces* **2013**, *5*, 4457.
40. Marambio-Jones, C.; Hoek, E. M. V. *J. Nanopart. Res.* **2010**, *12*, 1531.
41. Rinaldi, S.; Fortunati, E.; Taddei, M.; Kenny, J. M.; Armentano, I.; Latterini, L. *J. Appl. Polym. Sci.* **2013**, *130*, 1185.
42. Nocchetti, M.; Donnadio, A.; Ambrogi, V.; Andreani, P.; Bastianini, M.; Pietrellac, D.; Latterinia, L. *J. Mater. Chem. B* **2013**, *1*, 2383.
43. Xu, T.; Xie, C. S. *Prog. Org. Coat.* **2003**, *46*, 297.
44. Zhang, L.; Jiang, Y.; Ding, Y.; Povey, M.; York, D. *J. Nanopart. Res.* **2007**, *9*, 479.
45. Ma, X. Y.; Zhang, W. D. *Polym. Degrad. Stabil.* **2009**, *94*, 1103.
46. Li, L. H.; Deng, J. C.; Deng, H. R.; Liu, Z. L.; Li, X. L. *Chem. Eng. J.* **2010**, *160*, 378.
47. Kikuchi, Y.; Sunada, K.; Iyoda, T.; Hashimoto, K.; Fujishima, A. *J. Photochem. Photobiol. A* **1997**, *106*, 51.
48. Halliwell, B.; Gutteridge, J. M. C. *Biochem. J.* **1984**, *219*, 1.
49. Sclafani, A.; Mozzanega, M.; Pichat, P. *J. Photochem. Photobiol. A* **1991**, *59*, 181.
50. Zhou, G.; Deng, J. C. *Mater. Sci. Semicond. Process.* **2007**, *10*, 90.
51. Wu, D. Y.; Svazas, A. *J. Nanosci. Nanotechnol.* **2006**, *6*, 3919.
52. Wang, W. S.; Gao, B. J.; Jiang, Y. M.; Huang, X. Q. *Chem. Ind. Eng. Process.* **2007**, *26*, 554.
53. Nakagawa, H.; Sano, H. *Polym. Prep. (Am. Chem. Soc., Div. Polym. Chem.)* **1992**, *26*, 249.
54. Shi, J.; Wang, Y.; Gao, Y.; Bai, H. *Compos. Sci. Technol.* **2008**, *68*, 1338.